Bioorganic & Medicinal Chemistry 22 (2014) 616–622

Contents lists available at ScienceDirect

Bioorganic & Medicinal Chemistry

journal homepage: www.elsevier.com/locate/bmc

Fragment based discovery of arginine isosteres through REPLACE: Towards non-ATP competitive CDK inhibitors

Padmavathy Nandha Premnath [†], Shu Liu [†], Tracy Perkins, Jennifer Abbott, Erin Anderson, Campbell McInnes [*]

Drug Discovery and Biomedical Sciences, South Carolina College of Pharmacy, University of South Carolina, Columbia, SC 29208, United States

ARTICLE INFO

Article history:
Received 22 August 2013
Revised 16 October 2013
Accepted 24 October 2013
Available online 7 November 2013

Keywords:
Cyclin dependent kinase
Drug discovery
Inhibitor
Anti-tumor therapeutic
REPLACE

ABSTRACT

In order to develop non-ATP competitive CDK2/cyclin A inhibitors, the REPLACE strategy has been applied to generate fragment alternatives for the N-terminal tetrapeptide of the cyclin binding motif (HAKRRLIF) involved in substrate recruitment prior to phosphotransfer. The docking approach used for the prediction of small molecule mimics for peptide determinants was validated through reproduction of experimental binding modes of known inhibitors and provides useful information for evaluating binding to protein–protein interaction sites. Further to this, potential arginine isosteres predicted using the validated LigandFit docking method were ligated to the truncated C-terminal peptide, RLIF using solid phase synthesis and evaluated in a competitive binding assay. After testing, identified fragments were shown to represent not only appropriate mimics for a critical arginine residue but also to interact effectively with a minor hydrophobic pocket present in the binding groove. Further evaluation of binding modes was undertaken to optimize the potency of these compounds. Through further application of the REPLACE strategy in this study, peptide-small molecule hybrid CDK2 inhibitors were identified that are more drug-like and suitable for further optimization as anti-tumor therapeutics.

1. Introduction

CDKs associate with cyclins to regulate the cell cycle checkpoints and control cell proliferation.[1] CDK2/cyclin A (CDK2A) controls DNA replication through phosphorylation of the transcription factor E2F-1, the activity of which is often deregulated in tumor cells. Inhibition of CDK2A has been shown to selectively induce apoptosis of cancer cells through the E2F-1 pathway and therefore is an attractive target for controlling abnormal cell proliferation.[2,3] Currently, available CDK inhibitors primarily target the highly conserved ATP binding site and generally inhibit both cell cycle and transcriptional CDKs potentially leading to toxicities in normal cells.[3,4] In our present study we utilize an alternative approach to selectively inhibit cell cycle CDKs by targeting protein–protein interactions distinct from the ATP binding pocket. CDK complexes recruit substrates and endogenous inhibitory proteins through the cyclin binding groove (CBG) only in the cell cycle CDK context (CDK2/Cyclin A, E; CDK4/cyclin D).[5–7] The CBG is recognized by a conserved cyclin binding motif (CBM), has been truncated and optimized to potent octapeptides including HAKRRLIF,[8] and further minimized to small peptides retaining low micromolar binding affinity.[8,9] Arg4 of the 8mer is particularly important for activity since modification to even the uncharged isostere, citrulline leads to at least a 10 fold loss in binding.[8,9] In this present study, the REPLACE (Replacement with Partial Ligand Alternatives through Computational Enrichment) strategy has been applied to identify fragment based alternatives for the N-terminus of CBG-peptides and suitable mimetics for the critical arginine in order to convert the octamer to a less peptidic inhibitor.[10,11] Validation of the LigandFit docking method[12] was carried out as a prelude to computationally evaluating fragment alternatives. Predicted N-terminal capping groups were then incorporated as Fragment Ligated Inhibitory Peptides (FLIPs) through solid phase synthesis and after in vitro evaluation, furoic, phenyl acetic and picolinic acid derived groups were shown to inhibit binding to CDK2/cyclin A while improving the drug likeness. These compounds represent the basis for further optimization of cell cycle CDK inhibitors as preclinical candidates for cancer therapy.

2. Materials and methods

2.1. Computational chemistry

The parameters of the LigandFit (Discovery Studio 3.0, Accelrys) docking method were validated using ligands from cyclin A/CDK2 crystal structures. The crystallographic ligands 1-(3,5-dichlorophenyl)-5-methyl-1*H*-1,2,4-triazole-3-carbaldehyde (3,5-DCPT) (PDB ID: 2UUE) and 1-(4-chlorophenyl)-5-methyl-1*H*-1,2,4-triazole-3-carbaldehyde (4-CPT) (PDB ID: 2V22) were used as positive

* Corresponding author. Tel.: +1 (803) 576 5684.
E-mail address: mcinnes@sccp.sc.edu (C. McInnes).
† These authors made equal contributions to this manuscript.

0968-0896/$ - see front matter © 2013 Elsevier Ltd. All rights reserved.
http://dx.doi.org/10.1016/j.bmc.2013.10.039

controls and 5-chloro-2-phenyl-1,8*a*-dihydroimidazo[1,2-*a*]pyridine-3-carbaldehyde was evaluated as a negative control. The three ligands were docked successively into the cyclin grooves of two structures (2V22, 2UUE) and 20 poses were generated for each. This was repeated by variation of the LigandFit parameters including the forcefield used for the energy grid (Dreiding, CFF and PLP1), use of minimization sphere (on or off) and different scoring functions (Ligscore1_Dreiding, Ligscore2_Dreiding, PLP1, PLP2, PMF, DOCKSCORE) to determine which generated a calculated binding energy most predictive of the experimental binding mode. For each parameter and scoring function, the number of correct poses of the positive controls in the top 25 ranked binding modes (out of 60 possible, 20 for each of the three ligands) was determined. A library of 20 potential fragment alternatives was manually built using ChemDraw for Excel (Perkin Elmer) and subsequently imported into DiscoveryStudio 3.0 (Accelrys). For docking of unknown compounds, 10 poses were generated since this was sufficient to generate correct poses for the control ligands.

2.2. Chemistry

All the starting materials, solvents and reagents were used as obtained without further purification. Analytical thin layer chromatography was performed on silica gel (GF-254 plates). ^{1}H and ^{13}C NMR spectra were recorded with a Varian Mercury 300 and 400 Spectrometer, respectively. Mass spectra were measured with a Micromass QTOF (Tandem quadruple-time of flight mass spectrometer), electrospray ionization (ESI) and VG 70S (Double-focusing magnetic sector mass spectrometer, EI). Analytical purities of evaluated compounds were >95% unless stated otherwise. The following analytical method (unless stated otherwise) was used on a Waters Alliance 2695 HPLC with a 2996 diode-array detector and equipped with a C18 (2) 100 A, 250 × 4.6 mm, 5 μm column (Phenomenox Luna). A gradient from 100% water (0.1% trifluoroacetic acid) to 60% acetonitrile (0.1% trifluoroacetic acid) was run over 30 min and held for 4 min. The chromatograms were extracted at 226 and 254 nm.

2.2.1. Synthesis of capping groups

Furoic acid, picolinic acid and 2-(3,4-dihydroxyphenyl)acetic acid N-terminal capping groups were all obtained commercially (Chembridge, Matrix Scientific and UKROrgSyth). 3-Alkoxy phenyl acetic acid derivatives were synthesized using the following procedure.

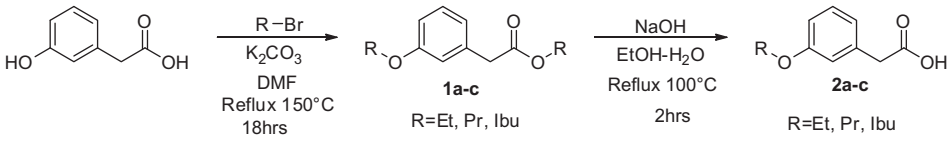

2.2.1.1. Step 1: Synthesis of ethyl 2-(3-ethoxyphenyl) acetate (1a)[13]. 3-hydroxyphenylacetic acid (0.76 g, 5 mmol), ethyl bromide (0.25 g, 23 mmol) and potassium carbonate (0.13 g, 16.5 mmol) were refluxed in 5 mL of DMF for 12–18 h. The reaction was monitored by TLC (ethylacetate:hexanes = 35:65), after the reaction was complete, the reaction mixture was cooled to room temperature; water was added to dissolve potassium carbonate. The aqueous layer was extracted with ethyl acetate and the combined organic layers were washed with saturated sodium bicarbonate, brine, dried over sodium sulfate and evaporated to yield a reddish oil (0.31 g, yield-30.0%).

^{1}H NMR (Chloroform-D, 300 MHz) δ (ppm) 7.13 (t, J = 7.32 Hz, 1H), 6.75 (t, J = 8.73 Hz, 3H), 4.06 (q, J = 7.80 Hz, 2H), 3.93 (q, J = 6.75 Hz, 2H), 3.50 (d, J = 7.26 Hz, 2H), 1.31 (t, J = 6.87 Hz, 3H), 1.16 (t, J = 7.02 Hz, 3H).

EI 208.

2.2.1.2. Propyl 2-(3-propoxyphenyl)acetate (1b). Reddish oil (yield-28.2%) ^{1}H NMR (Chloroform-D, 300 MHz) δ (ppm) 7.25–7.19 (m, 1H), 6.83 (t, J = 8.07 Hz, 3H), 4.05 (t, J = 6.78 Hz, 2H), 3.91 (t, J = 6.39 Hz, 2H), 3.59 (d, J = 6.96 Hz, 2H), 1.80 (q, J = 7.35 Hz, 2H), 1.64 (q, J = 6.00 Hz, 2H), 1.03 (t, J = 7.32 Hz, 3H), 0.91 (t, J = 7.33 Hz, 3H).

EI 224.

2.2.1.3. Isobutyl 2-(3-isobutoxyphenyl)acetate (1c). Reddish oil (yield-24.2%) ^{1}H NMR (Chloroform-D, 300 MHz) δ (ppm) 7.22 (t, J = 8.34 Hz, 1H), 6.85–6.79 (m, 3H), 3.89 (d, J = 6.48 Hz, 2H), 3.71 (d, J = 6.93 Hz, 2H), 3.60 (s, 2H), 2.12–2.03 (m, 1H), 1.97–1.88 (m, 1H), 1.03 (d, J = 6.18 Hz, 6H), 0.92 (d, J = 6.60 Hz, 6H).

EI 264.

2.2.1.4. Step 2: 2-(3-Ethoxyphenyl) acetic acid (2a)[13]. The ethyl 2-(3-ethoxyphenyl) acetate (1.41 g, 5 mmol) obtained from step 1 was treated with sodium hydroxide (2.8 g, 70 mmol) and a solution of 15 mL ethanol and 15 mL water. The reaction mixture was refluxed for 2 h and the reaction was monitored by TLC (ethylacetate:hexanes = 35:65). After the completion of reaction, the reaction mixture was cooled, the alcohol was evaporated and diluted with water. The reaction mixture was acidified with 1 N hydrochloric acid and stirred to precipitate the product as white solid (0.73 g, yield-81.2%).

^{1}H NMR (chloroform-D, 500 MHz) δ (ppm) 7.28–7.24 (m, 1H), 6.88–6.83 (m, 3H), 4.05 (q, J = 6.80 Hz, 2H), 3.63 (s, 2H), 1.42 (t, J = 7.25 Hz, 3H).

^{13}C NMR (chloroform-D, 125 MHz) δ (ppm) 177.15, 159.14, 134.61, 129.60, 121.55, 115.65, 113.41, 63.41, 41.01, 14.80.

EI 180.

2.2.1.5. 2-(3-Propoxyphenyl)acetic acid (2b). White solid (yield-85.2%) ^{1}H NMR (chloroform-D, 300 MHz) δ (ppm) 7.21(d, J = 7.44 Hz, 2H), 6.83 (t, J = 7.86 Hz, 2H), 3.90 (t, J = 6.03 Hz, 2H), 3.61 (s, 2H), 1.79 (q, J = 6.42 Hz, 2H), 1.02 (t, J = 7.05 Hz, 3H).

EI 194.

2.2.1.6. 2-(3-Isobutoxyphenyl)acetic acid (2c). White solid (yield-82.8%) ^{1}H NMR (chloroform-D, 300 MHz) δ (ppm) 7.22 (d, J = 8.19 Hz, 1H), 6.83 (t, J = 8.70 Hz, 3H), 3.70 (d, J = 7.26 Hz, 2H), 3.62 (s, 2H), 2.11–2.00 (m, 1H), 1.01 (d, J = 6.69 Hz, 6H).

EI 208.

2.2.2. Peptide and FLIP synthesis

Unless otherwise indicated, capping groups were obtained commercially from ChemBridge and UORSYS and were used as provided. Peptides were assembled by using standard solid-phase synthesis methods.[10] A sample procedure is given as follows: 5 equiv of the C-terminal amino acid were coupled to Rink resin at the first place using DIEA (0.082 mL) and HBTU (189.6 mg) in 5 mL of DMF for 1 h. The Fmoc of the C-terminal amino acid was removed using 20% piperidine in 5 mL of DMF for 10 min before addition of 5 equiv of the next amino acid using DIEA (0.082 mL) and HBTU (189.6 mg) in 5 mL of DMF. Wash cycles (5 × 10 mL of DMF + 5 × 10 mL of DCM) were applied to each step in

between coupling and deprotection of Fmoc. Upon completion of assembly, side chain protecting groups were removed, and FLIPs were cleaved from Rink resin using 90:5:5 mixtures of TFA/H_2O/TIPS. Crude FLIPs were purified using reverse-phase flash chromatography and semi preparative reverse-phase HPLC methods. Pure compounds were lyophilized and characterized using mass spectrometry and analytical HPLC (see Supplementary Table 1).

2.3. Fluorescent polarization binding assay

2.3.1. CDK4D1 FP assay

This assay was performed using black 384-well plates using a previously described procedure[14] with the following modifications. To each well were added: 5 μl CDK4D1 (0.3 μg/well purified recombinant human kinase complex from Invitrogen), 5 μl compound solution, 5 μl 30 nM fluoresceinyl-Ahx-Pro-Val-Lys-Arg-Arg-Leu-(3ClPhe)-Gly tracer peptide. Compounds and kinase complexes were diluted using assay buffer (25 mM HEPES pH 7, 10 nM NaCl, 0.01% Nonidet P-40, 1 mM dithiothretiol). The plate was centrifuged for 1 min at 500 rpm and then incubated with shaking for 45 min at room temperature. Fluorescence polarization was measured on a DTX880 multimode detector (Beckman Coulter, Brea, CA) fitted with 485/535 nm excitation/emission filters and a dichroic mirror suitable for fluorescein. Relative mp was calculated for each concentration tested using the equation showing below. IC_{50} values were determined by logarithmic regression by correlating mean polarizations (mp) and testing concentrations.

$$\text{Relative mean polarization(RMP)} = \frac{\text{mP(compound)} - \text{mP(DMSO, protein, tracer)}}{\text{mP(DMSO, protein)} - \text{mP(DMSO, protein, tracer)}}$$

2.3.2. CDK2A2 FP assay

This assay was performed using black 384-well plates. To each well were added: 5 μl CDK2A2 (0.3 μg/well purified recombinant human kinase complex), 5 μl compound solution, 5 μl 30 nM fluoresceinyl-Ahx-Pro-Val-Lys-Arg-Arg-Leu-Phe-Gly tracer peptide. Compounds and kinase complexes were diluted using assay buffer (25 mM HEPES pH 7, 10 nM NaCl, 0.01% Nonidet P-40, 1 mM dithiothretiol). The plate was centrifuged for 1 min at 500 rpm and then incubated with shaking for 45 min at room temperature. Fluorescence polarization was read on a DTX880 multimode detector (Beckman Coulter, Brea, CA) fitted with 485/535 nm excitation/emission filters and a dichroic mirror suitable for fluorescein. Relative mp was calculated for each concentration tested using the equation showing below. IC_{50} values were determined by logarithmic regression by correlating mean polarization (mp) and testing concentrations.

$$\text{Relative mean polarization(RMP)} = \frac{\text{mP(compound)} - \text{mP(DMSO, protein, tracer)}}{\text{mP(DMSO, protein)} - \text{mP(DMSO, protein, tracer)}}$$

3. Results

3.1. Validation of REPLACE docking method

Validation of the method used for computational aspects of REPLACE was undertaken to demonstrate that docking results obtained for unknown compounds would be predictive of their in vitro activity. In addition, docking methods generally are specific for a particular binding site and therefore require judicious selection. Furthermore, protein–protein interactions are known to be difficult to study through computational analysis and therefore validation exercises would provide insights into the best force-fields and scoring functions for these. To achieve this, the N-terminal capping groups (Ncaps) from the crystal structures of two FLIPs bound to CDK2A (1-(3,5-dichlorophenyl)-5-methyl-1*H*-1,2,4-triazole-3-carboxamide-Arg-Leu-Ile-4-fluoroPhe (3,5-DCPT) (PDB ID: 2UUE) and 1-(4-chlorophenyl)-5-methyl-1*H*-1,2,4-triazole-3-carboxamide-Arg-Leu-Ile-4-fluoroPhe) (4-CPT) (PDB ID: 2V22) were used as positive controls while an inactive compound 5-chloro-2-phenyl-1,8*a*-dihydroimidazo[1,2-*a*]pyridine-3-carbaldehyde was evaluated as negative control.[10]

The Ncap positive controls (3,5-DCPT and 4-CPT) when bound to the CBG make important hydrogen bonding interactions with residues Gln254 and Trp217.[10] To determine if the docking method used (LigandFit, DiscoveryStudio) is predictive in terms of reproducing experimental binding modes, the docked poses of the 3,5-DCPT and 4-CPT with 2UUE were examined for similar orientation of the aromatic and triazole rings and also retention of the two hydrogen bonding interactions. Reproducibility of the docking method was assessed through examining the number of correct poses (i.e., those superimposable with the crystal structure) or close poses (poses that show a RMSD value $\leqslant$2.0 Å) with the crystal structure) of the positive control ligands generated and the number of negative control poses in top the 25 ranked conformations (20 poses generated for each ligand, 60 in total). This was repeated for both cyclin subunits (B and D) observed in the asymmetric unit of the crystal structure. The result for subunit B showed 10 and 14 correct/close poses of 3,5-DCPT and 4-CPT whereas those for subunit D showed only 11 close poses of 4-CPT and no correct/close poses for 3,5-DCPT. There were no poses of the negative control in the top 25 poses for either subunit. Due to the better data obtained for subunit B, this was considered for further parameter optimization. For each energy grid available in LigandFit, the number of top ranked correct/close poses was calculated for each scoring function (Ligscore1_Dreiding, Ligscore2_Dreiding, PLP1, PLP2, Jain, PMF and DOCKSCORE). The Dreiding, CFF and PLP1 energy grids generated 2, 4 and 6 correct poses (in the top 25 ranked) respectively for 3,5-DCPT for the best scoring function. There were 18 and 15 poses of the negative control ligands generated using Dreiding and CFF grids, respectively, however none were observed for the PLP1 method in top 25 ranked compounds and therefore indicating this as the most successful for this validation (Table 1). Further analysis of the docked poses revealed that the most effective scoring function was determined to be PLP1 since it resulted in 9 and 6 correct or close poses for 3,5-DCPT and 4-CPT, respectively. The optimized docking protocol was therefore found to include use of the PLP1 energy grid, and the PLP1 scoring function with 10 poses generated for each structure. These results demonstrated full validation of the docking approach and strongly suggest that results obtained with unknown ligands will be predictive.

A library of compounds based on the native ligand (1-(3,5-dichlorophenyl)-5-methyl-1*H*-1,2,4-triazole-3-carbonyl and the parent peptide (HAKRRLIF) was designed to include pharmacophoric features observed in this series. A library of 20 compounds was built on core scaffolds including phenylacetic acids, five-membered heterocyclic analogs, and also picolinic acid derivatives. These fragments were designed to interact with Trp217 and Gln254 through H-bonds, the secondary hydrophobic pocket (alkyl/aryl group for van der Waals interaction), and the acidic region (heterocyclic and/or amine groups) through ion-pairing interactions with Glu224/Glu220. Phenyl acetic acid derivatives were designed with alkoxy groups at position 3 and/or 4 to make van der Waals

Table 1
Optimization of docking parameters for LigandFit method

Positive control

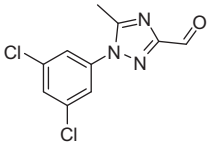

35DCPT

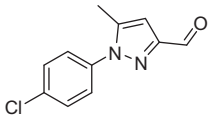

4CPT

Negative control

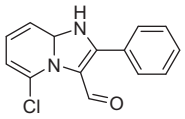

Energy grid	Dreiding	CFF	PLP1
No. of correct poses 3,5-DCPT	2	4	6
No. of correct poses 4-DCPT	—	—	8
No. of negative control poses in top 25	–PLP1(4), –PLP2(4), Jain (4), PMF(4), DOCK SCORE(6)	–PMF (7), DOCK SCORE (6)	0
Best scoring functions	LigScore2	PLP1, PLP2	PLP1, PLP2
3,5-DCPT (rank of top 25 correct/closer poses for the best scoring function)	4,5 (For all the scoring functions)	PLP1(9–12, 25), PLP2(13–16, 25)	PLP1(7–10, 14, 11–13, 25) PLP2(11–18)
4-DCPT (rank of top 25 correct/closer poses for the best scoring function)	—	PLP1 (1–8), PLP2(17–24)	PLP1(1–6), PLP2(20–25)

interactions with the secondary pocket. Picolinic acid derivatives were substituted at the 3 position in order to interact with the alanine pocket and this series also included basic substitutions at the 4 position (guanidinomethyl, diethyl aminomethyl, piperazinylmethyl) for ion-pairing interactions. In addition, five-membered heterocycles included 1,2,4-triazole, pyrazole, furan, pyrrole and thiophene carboxylic acid were substituted with another heterocyclic ring structure (including imidazole, pyrazole, thiophene). Other modifications of the furan carboxylic acid included addition of diethylaminomethyl and piperazinylmethyl groups selected as arginine isosteres due to their potential for ion-pairing interactions.

The binding site for the potential capping groups was created by deletion of the N-terminus of the crystallographic ligand from the CBG. After generation of the site points, fragment alternatives were docked using the optimized LigandFit parameters. Docked fragments were analyzed and shortlisted based on the required interactions, PLP1 scoring, and correct positioning of the carbonyl for H-bonding. The interactions of **5856** (PLP1 score = −35.03), **5581** (PLP1, -52.1) bound to the cyclin A groove are shown in Figure 1 and **5589** (PLP1, -42.61) in the cyclin D groove are shown in Figure 2.

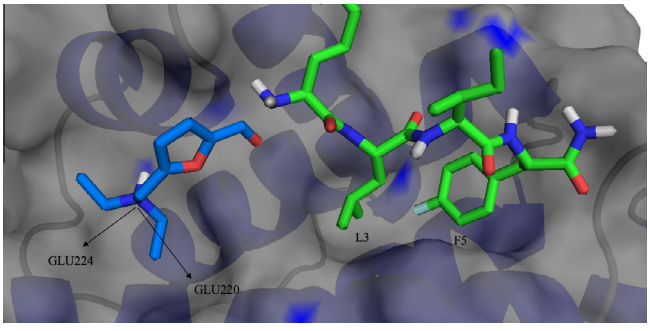

Figure 1. Docked pose of the Ncap for **5581** (blue carbons) with cyclin A (grey Connolly surface; 2V22) illustrating how the fragment alternatives are generated. Cyclin residues are labeled as three letter amino acid codes whereas peptide residues as one letter codes. The peptidic component retained during the docking is shown with green carbons. **5581** interacts both with the secondary hydrophobic pocket (through the right hand aminoethyl group) and through ion pairing interactions with Glu220 and Glu224.

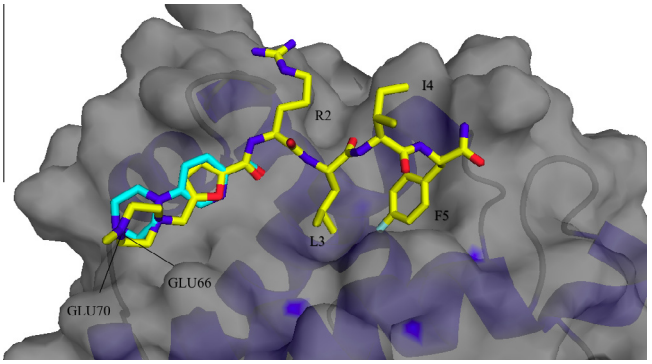

Figure 2. Modeled structures of **5856** (cyan ligand) and **5589** (yellow ligand) in complex with cyclin D1 (grey Connolly surface; 2W96). Cyclin residues are labeled as three letter amino acid codes whereas peptide residues as one letter codes. Favorable interactions between acidic residues of the cyclin (Glu 66 and 70) and the piperazinylmethyl group of the inhibitor are represented by solid lines.

3.2. Structure–activity relationship of furoic and thiazole carboxylic acid derivatives as N-Cap core structures

We have previously described Fragment Ligated Inhibitory Peptides (FLIPs) with comparable potency to the native p21 pentapeptide (RRLIF) in binding to CDK2/cyclin A (CDK2A) and CDK4/cyclin D1 (CDK4D1) complexes.[15] CDK4/cyclin D1 is another cell cycle regulatory kinase that controls the G1/S transition and is a validated cancer target. The capping groups described were phenylheterocyclic core structures as alternatives for the N-terminal residues and resulted in inhibitors with more drug-like properties including more optimal *C* log *P* values and polar surface area.[15] Relative to the CDK4D1 activity of this pentapeptide, a significant potency increase was obtained for phenyltriazole FLIPS. Binding of the N-caps to the secondary hydrophobic pocket occurs through van der Waals interactions with the phenyl ring bypassing the arginine binding site.[6] Potential for ion pairing interactions made by the N-terminal residues of the peptide (HAKR), have therefore not been fully exploited in the design of partial ligand alternatives. Appropriate substitution of a heterocyclic scaffold would allow complementarity with both the secondary hydrophobic pocket of the groove and the acidic residues that surround this subsite. This would build on the previous Ncaps where interaction of the phe-

nyltriazole rings (and pyrazole) occurs primarily through van der Waals contacts with the alanine pocket. To achieve these additional interactions, functional groups including *N*,*N*-diethylaminomethyl, pyrazolylmethyl and piperazinylmethyl groups were selected from docking results and incorporated in the furoic acid context in order to simultaneously interact with both subsites of the cyclin. To facilitate synthetic accessibility, these were initially pursued in the context of furoic acid and thiazole-4-carboxylic acid core structures as a scaffold to present requisite functionality both to the secondary hydrophobic pocket and to the acidic region of the CBG.

A series of furoic acid and thiazole-4-carboxylic acid analogs were therefore incorporated into FLIPs and evaluated as capping group replacements for the N-terminus of the octapeptide. The capping groups were ligated to the RLIF tetrapeptide and their activity compared to the pentapeptide with the native arginine residue (RRLIF) through testing in a fluorescence polarization competitive binding assay (Table 2). Although this assay does not provide a readout of functional kinase activity, previous comparisons have shown that there is a close correlation between competitive binding and inhibition of CDK functional activity through the cyclin groove.[8,14] Of the FLIP analogs synthesized and tested, the *N*-ethyl-*N*-methylethanamine analog (**5581**) proved to be the most potent compound in this series not only against CDK2A2 (43.5 μM) but also against CDK4D1 (41.9 μM). The 1-ethyl-1*H*-imidazole analog (**5585**) and 1-ethyl-4-methyl-1*H*-pyrazole analog (**5761**) only showed modest activities for CDK2A with IC_{50} values falling to 100 μM. Both the methyl and des-methyl pyrazole analogs (**5761**, **5586**) were shown to be weak binders to CDK2A2 with IC_{50} values between 100 and 180 μM. The (4-methylpiperazin-1-yl)methyl analog (**5589**) was shown to have similar respectable activity against CDK2A2 and CDK4D1 (IC_{50} = 50.3 and 43.2 μM, respectively), with its potency being within 2–3-fold that of RRLIF (16.1 μM). The IC_{50} value for the imidazole methyl analog (**5585**) for CDK4D1 was approximately 150 μM; slightly weaker than its CDK2A2 activity. The pyrazole Ncap analogs (**5586** and **5761**) were determined to have IC_{50} values greater than 100 μM. The affinity of the thiazole-4-carboxylic acid analog with a 3-thienyl substitution (**5582**) was at least three times greater than that of the 2-thienyl analog (**5584**, 56.2 μM vs >180 μM) in the CDK2A2 assay.

3.3. Structure–activity relationship of picolinic acid and phenylacetic carboxylic acid derivatives as N-Cap core structures

In addition to the core structures described above, two alternative scaffolds were investigated. Fragment alternatives containing picolinic acid and phenylacetic acid substructures were employed in order to mimic the HAKR binding site. As observed in the phenylheterocyclic series, a critical hydrogen bond is formed between the N2 of the 1,2,4 triazole and indole NH of Trp217 of cyclin A.[10] Structural comparison of triazole and picolinic acid core structures indicate that the pyridine ring of the picolinic acid would present an H-bond acceptor in a similar position to the N2 of the triazole and thus represents a viable alternative scaffold.

Picolinic acid derivatives were designed in order to incorporate substituents interacting with either the secondary hydrophobic pocket or the arginine binding site. R1 substituents including, methyl (**5845**), methoxy (**524**) and ethoxy (**523**) substitutions (6 position) and at R2, a piperazine substitution (**5856**) was incorporated (Table 3). Analogs were synthesized in the RLNpfluorophenylalanine (RLNpfF) or RLIF contexts with the former having a slightly greater affinity as a pentapeptide.[8] After testing in the competitive binding assays, the unsubstituted analog (**525**) was found to have an IC_{50} of 29.2 μM against CDK2A. Both the 6-methyl (**5845**) and 6-methoxy (**524**) substitutions resulted in decreased potency with IC_{50}s of >100 and 36.4 μM, respectively. The 6-ethoxy containing FLIP (**523**) was determined to have an IC_{50} of 39.7 μM suggesting that affinity was not gained through substitution at R1. In the CDK2A context, the 5-piperazine derivative (**5856**) did not increase the binding affinity relative to **525** as the IC_{50} was determined to be approximately 100 μM. This analog did however exhibit increased potency relative to **525** in the CDK4D1 (two-fold,

Table 2
Structure activity of 2-furoic acid and thiazole-4 carboxylic acid FLIPS

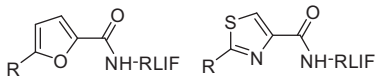

1 **2**

SCCP ID	R	Core		CDK2/cyclin A IC_{50} (mM)	CDK4/cyclin D1 IC_{50} (mM)
5581	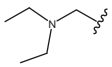	1	—	43.5 ± 1.2	41.9 ± 3.1
5585	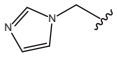	1	—	>100	158.6 ± 5.2
5586	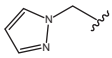	1	—	>100	>100
5589	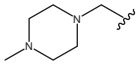	1	—	50.3 ± 1.3	43.2 ± 5.0
5761	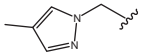	1	—	>100	>180
5582		—	2	56.2 ± 1.2	>180
5584		—	2	>180	>180

Table 3
Structure activity of picolinic acid FLIPs

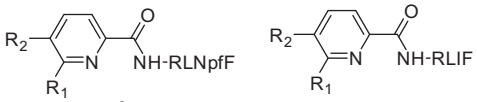

SCCP ID	R1	R2	Core		CDK2/cyclin A IC_{50} (mM)	CDK4/cyclin D1 IC_{50} (mM)
525	H	H	1	—	29.2 ± 1.3	48.4 ± 1.2
5845	Me	H	—	2	>100	85.7 ± 1.9
524	MeO	H	1	—	36.4 ± 1.2	36.9 ± 1.4
523	EtO	H	1	—	39.7 ± 1.2	>100
5856	H	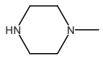	—	2	>100	21.9 ± 1.1

IC_{50} = 21.9 μM). The 6-methyl (**5845**) and 6-ethoxy (**523**) analogs were weaker inhibitors than **525** and **5856** for CDK4D1 however the 6-methoxy derivative (**524**) had a slight potency increase to 36.9 μM compared to both of these FLIPs.

In a further series of N-terminal capping groups, the presence of a bridging methylene between the linking carboxylate group and the aryl ring was explored through the synthesis of phenylacetic acid Ncaps so as to optimize interactions with the secondary lipophilic pocket. The SAR of four derivatives was determined in both CDK binding assays (Table 4) and revealed that a 3,4-diethoxy analog (**530**) was found to be the most potent against both CDK2A2 and CDK4D1 (5.2 μM vs 3.0 μM). Single R1 substitutions were explored and included ethoxy (**5854**), *n*-propyloxy (**5853**), and isobutoxy (**5855**). None of these analogs in the FLIP context possessed appreciable binding affinity in either assay.

4. Discussion

Prior to docking unknown fragments into the cyclin groove, the LigandFit method was validated with known partial ligand alternatives. For docking methods in general, the binding affinity of a ligand is estimated by a scoring function which evaluates the receptor–ligand interactions. The PLP energy grid and scoring functions were found to be the most effective for reproducing the experimental binding mode of the 35DCPT and 4CPT N-terminal capping groups (Table 1). Of the scoring functions used, only PLP1 and PLP2 explicitly estimate contributions from hydrogen bonding.[12] Previous SAR has demonstrated that H-bonding to Trp217 and Gln254 of cyclin A are critical interactions of a potential ligand,[15] therefore suggesting why the PLP functions are the most effective. This result indicates that the LigandFit docking protocol with the PLP energy grid and scoring function would be a beneficial strategy in application to protein–protein interactions which typically involve numerous interactions including multiple H-bonds. Further to this validation, LigandFit was used to evaluate binding modes of new fragment alternatives for the N-terminal tetrapeptide of HAKRRLIF. Using this computational approach, fragment ligated inhibitory peptides containing various N-cap structures (5-furoic acid, thiazole-4-carboxylic acid, 5 and 6 substituted picolinic acids and 3 and 4 substituted phenylacetic acids) were designed with the purpose of reproducing interactions with CBG observed in peptidic inhibitors. After solid phase synthesis, the inhibitory activity of these compounds against both CDK2A and CDK4D1 was determined using an FP competitive binding assay to generate SAR information useful in the development of potential cell cycle specific inhibitors. As a whole, scoring functions used in high-throughput docking are qualitative and are used to differentiate binders from nonbinders. It is therefore not surprising that no correlation was observed between the PLP1 scoring values calculated in these REPLACE iterations and the observed IC_{50} values.

Table 4
Structure activity of Phenylacetic acid FLIPs

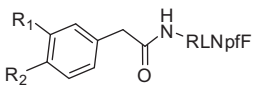

SCCP ID	R1	R2	CDK2/cyclin A IC_{50} (mM)	CDK4/cyclin D1 IC_{50} (mM)
5854	H	EtO	>100	>100
5853	H	$CH_3CH_2CH_2O$	>100	>50
5855	H	$(CH_3)_2CHCH_2O$	>100	>100
530	EtO	EtO	5.2 ± 1.1	3 ± 1.4

The most potent furoic acid based N-caps identified for both CDK2A and CDK4D1 contained either a diethylaminomethyl or a piperazinylmethyl group. Both of these derivatives would be positively charged at physiological pH, therefore indicating the importance of establishing ionic interactions with E220 (E66 in cyclin D1) and thus confirming that they are reasonable mimics for the native peptide arginine. The structural basis for the similar potency observed with **5581** (Fig. 1) and **5589** (Fig. 2) for CDK2A and CDK4D1 can be explained analyzing the cyclin contact residues in each context. Both cyclin A and D have an acidic region (Glu220, Glu224 in cyclin A, Glu66 in cyclin D) that interacts with the arginine residue. The charged basic substituents of the two capping groups therefore interact effectively with this acidic region through ion pairing contacts. In addition, the ethyl groups of **5581** interact with the minor hydrophobic pocket of the cyclin groove providing additional affinity for the CDK complexes studies (Fig. 1). Although the 3-thienyl (**5582**) and 2-thienyl (**5584**) derivatives both contain a similar heterocyclic moiety, **5582** displays increased activity probably due to the secondary hydrophobic pocket in the cyclin A context which is able to accommodate the larger sulfur atom in the relevant position of thiophene ring.

Comparison of the activity of the furoic acid derived FLIPs with the phenylfuroic acid derivatives previously described suggests that introduction of basic substituents results in significantly more potent cyclin groove inhibitors. The significant activity of **5581** and **5589** indicates the increased contribution of the dimethylaminomethyl group relative to the phenyl substituent. In addition, due to the increased H-bonding ability of the triazole system relative to the furan, phenyltriazole substituted FLIPs are about 100-fold more active. Future design efforts should combine substitutions (i.e., from **5581**, **5589**) onto a 1,2,4 triazole and therefore should generate more potent CDK inhibitors.

The observed activity for **525** and the increase in potency obtained for **5856** suggests that the picolinic acid scaffold is a viable one for further development and especially in the CDK4D1 context where addition of the piperazine to the aryl ring leads to increased activity. Binding is more favorable in the CDK4D1 scenario since the charged nitrogen is in closer proximity to E66 in this context and is able to closely mimic the interactions of Arg4 (Fig. 2). The increased activity of the 6-methoxy derivative (**524**) and the decreased potency of the 6-ethoxy (**523**) relative to the unsubstituted picolinic acid version suggests that there is an optimal size of the substituent for complementarity with the secondary hydrophobic pocket and that steric clashes with Trp217 limit the placement of larger groups on the aromatic ring. Furthermore the results obtained for the phenylacetic acid Ncap (most potent Ncap identified in this study) indicate the high potential of this scaffold for further development. Modeling of the diethoxy analog (**530**) concludes that only one of the substituents interacts with the minor pocket of the cyclin groove while the other one limits the conformational space available for the Ncap and therefore provides an entropic advantage for binding. Placement of similar basic functional groups to those in the furoic acid context instead of the 4-ethoxy substituent should provide increased affinity relative to **530**.

As a whole, these results demonstrate that N-cap core structures containing furoic acid, thiazole acid, picolinic acid and phenylacetic acid represent viable mimetics for the critical arginine residue and other determinants of potent cyclin groove binding. A computational docking approach was validated as a useful approach for predicting protein–protein interaction inhibitors and provided partial ligand alternatives that interact with both the minor hydrophobic pocket and the acidic region of the CBG. Synthesis of FLIP hybrid compounds based on the predicted structures validated the hypothesis that this approach would provide increased affinity relative to previous inhibitors that only interact with the minor pocket alone. Overall, a greater relative potency increase for FLIP inhibitors was observed for CDK4D1 than for CDK2A compared to the native pentapeptide (RRLIF) for a number of compounds and with potential improvement of their drug-like properties. These compounds therefore more completely mimic the contacts of the optimized peptide and are useful for further conversion to nonATP competitive CDK inhibitors for development as anti-tumor therapeutics.

Acknowledgments

We thank Dr's. Michael Walla and William Cotham in the Department of Chemistry and Biochemistry at the University of South Carolina for assistance with Mass Spectrometry, Helga Cohen and Dr. Perry Pellechia for NMR spectrometry. This work was funded by the National Institutes of Health through the research project Grant, 5R01CA131368.

Supplementary data

Supplementary data associated with this article can be found, in the online version, at http://dx.doi.org/10.1016/j.bmc.2013.10.039.

References and notes

1. Sherr, C. J. *Science* **1996**, *274*, 1672.
2. Chen, Y. N.; Sharma, S. K.; Ramsey, T. M.; Jiang, L.; Martin, M. S.; Baker, K.; Adams, P. D.; Bair, K. W.; Kaelin, W. G., Jr. *Proc. Natl. Acad. Sci. U.S.A.* **1999**, *96*, 4325.
3. Shapiro, G. I. *J. Clin. Oncol.* **2006**, *24*, 1770.
4. McInnes, C. *Drug Discovery Today* **2008**, *13*, 875.
5. Zheleva, D. I.; McInnes, C.; Gavine, A. L.; Zhelev, N. Z.; Fischer, P. M.; Lane, D. P. *J. Pept. Res.* **2002**, *60*, 257.
6. McInnes, C.; Andrews, M. J.; Zheleva, D. I.; Lane, D. P.; Fischer, P. M. *Curr. Med. Chem. Anticancer Agents* **2003**, *3*, 57.
7. Kirkland, L. O.; McInnes, C. *Biochem. Pharmacol.* **2009**, *77*, 1561.
8. Kontopidis, G.; Andrews, M. J.; McInnes, C.; Cowan, A.; Powers, H.; Innes, L.; Plater, A.; Griffiths, G.; Paterson, D.; Zheleva, D. I.; Lane, D. P.; Green, S.; Walkinshaw, M. D.; Fischer, P. M. *Structure* **2003**, *11*, 1537.
9. Kontopidis, G.; Andrews, M. J.; McInnes, C.; Plater, A.; Innes, L.; Renachowski, S.; Cowan, A.; Fischer, P. M. *ChemMedChem* **2009**, *4*, 1120.
10. Andrews, M. J.; Kontopidis, G.; McInnes, C.; Plater, A.; Innes, L.; Cowan, A.; Jewsbury, P.; Fischer, P. M. *Chembiochem* **1909**, *2006*, 7.
11. McInnes, C. In *Annual Reports in Medicinal Chemistry* In ; Bernstein, P., Desai, M., Eds.; Elsevier, 2012; Vol. 47, p 459.
12. Venkatachalam, C. M.; Jiang, X.; Oldfield, T.; Waldman, M. *J. Mol. Graphics Modell.* **2003**, *21*, 289.
13. Guy, S.; Yacine, P. J.; Jean, M. *Tetrahedron* **2003**, *59*, 3315.
14. Andrews, M. J.; McInnes, C.; Kontopidis, G.; Innes, L.; Cowan, A.; Plater, A.; Fischer, P. M. *Org. Biomol. Chem.* **2004**, *2*, 2735.
15. Liu, S.; Premnath, P. N.; Bolger, J. K.; Perkins, T. L.; Kirkland, L. O.; Kontopidis, G.; McInnes, C. *J. Med. Chem.* **2013**, *56*, 1573.